Noise Spectroscopy As A Tool For The Characterization Of Perovskite, Organic And Silicon Solar Cells

G. Landi[1,2,a)], C. Barone[3], C. Mauro[3], H. C. Neitzert[1] and S. Pagano[3]

[1]*Department of Industrial Engineering, University of Salerno, 84084 Fisciano, Italy*
[2]*Institute for Polymers, Composites and Biomaterials, National Research Council of Italy, 80055 Portici, Italy*
[3]*Dipartimento di Fisica "E.R. Caianiello" and CNR-SPIN Salerno, Università di Salerno, 84084 Fisciano, Italy*

[a)]Corresponding author: glandi@unisa.it

Abstract. Low-frequency noise spectroscopy has been used to monitor electronic properties of solar cells under temperature or radiation stress. For all the investigated polymer:fullerene, silicon and perovskite solar cells this technique evidences a clear correlation of the recombination and the transport processes with the device performances.

INTRODUCTION

Low-frequency noise spectroscopy has been used in order to evaluate transport properties and degradation processes in polymer:fullerene solar cells [1], polymer/carbon nanotube composites [2] and polymer transistors.[3] Hsu was the first to relate the 1/f-type noise in the p-n junctions to the fluctuation of the defect state population.[4] In the present study, noise spectroscopy has been applied to evaluate the carrier dynamics and degradation phenomena in different photovoltaic devices.[5-8]

DEVICE AND STRESS PROCEDURE DESCRIPTION

The noise measurements were performed as a function of the temperature, the bias current, and the illumination conditions. The solar cells were biased with a low-noise Keithley "220" dc current source and the output ac voltage signal was analyzed by using a dynamic signal analyzer "HP35670A". The investigated organic solar cell is based on a blend between poly(3-hexylthiophene) (P3HT) and [6,6]-phenyl-C6l-butyric acid methyl ester (PCBM). For more details on the device fabrication see.[1] The silicon solar cells are commercial boron-doped Czochralski based c-Si homojunction solar cells, whereas, the perovskite solar cell is based on $CH_3NH_3PbI_3$ as absorber. For a detailed description of the device preparation for the perovskite solar cell the reader is referred to. [8] In the case of the crystalline silicon solar cells, additional defects were artificially induced in the silicon layers by irradiation with 65 MeV protons (with a fluence of 5×10^{12} protons/cm^2).[6]

RESULTS AND DISCUSSION

The equivalent impedance of the solar cell can be modeled at low frequencies as a parallel connection between a fluctuating resistance $R_x(t)$ and a capacitance C_x [1]. $R_x(t)$ can be expressed as the sum of a constant average and a small fluctuating random function: $R_x(t) =< R_x > +\epsilon_R(t)$. In particular, the mean value corresponds to the differential resistance R_{rec}, defined as $R_{rec} = (dV_F/dI_{DC})$. Here I_{DC} is the dc bias current, $V_F = V_{DC} - I_{DC}R_S$ is the forward voltage without the effect of the series resistance and C_x is the sum of the geometrical capacitance and the chemical capacitance C_μ. Under forward bias the capacitance C_μ, related to the minority charge carriers accumulated into active layer, becomes dominant compared to the geometrical contribution C_g. [9] Therefore, the equivalent ac impedance is simplified to a parallel connection between the R_{rec} and C_μ. Since the fluctuations of $R_x(t)$ are the source of the voltage noise $S_V(f)$ within the device, the voltage noise spectra can be expressed as $S_V(f) = S_R(f)I_{DC}^2$.

The 3rd International Conference on Optoelectronic and Nano Materials for Advanced Technology (icONMAT 2019)
AIP Conf. Proc. 2082, 020001-1–020001-4; https://doi.org/10.1063/1.5093818
Published by AIP Publishing. 978-0-7354-1812-7/$30.00

[10] In the frequency domain this contribution is of 1/f-type noise given by $S_R(f) = KR_{rec}^2 f^{-\gamma}$, where K is the noise amplitude and γ is an exponent close to unity. [10] Therefore, it follows that

$$S_V(f) = \frac{K}{f^{\gamma}} \frac{R_{rec}^2 I_{DC}^2}{1+(f/f_x)^2}, \quad (1)$$

where $f_x = \left(2\pi R_{rec} C_{\mu}\right)^{-1}$ is the cut-off frequency, observed in the noise spectra.

Characterization of polymer:fullerene solar cell by using noise analysis

In order to investigate the influence of the solvents on film ordering within the active layer, noise spectroscopy has been performed on solar cells prepared with different solvent mixtures. In Figure 1 (a) the voltage spectral traces measured, at 300 K nin dark conditions with a bias current of 30 μA, for the solar cells fabricated with the reference oDCB solvent and with oDCB+THN are shown.

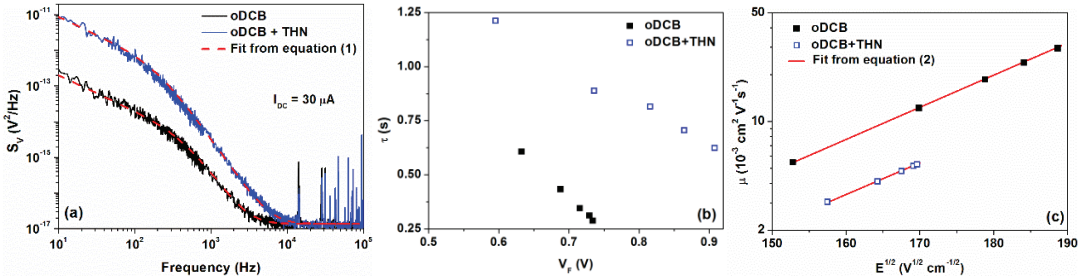

FIGURE 1. (a) Frequency dependence of the voltage-spectral densities measured at 30 μA for the device fabricated with oDCB (black solid line) and oDCB+THN (blue solid line). (b) Experimental electron lifetime dependence on V_F and (c) electron mobility dependence on $E^{1/2}$ for solar cells fabricated with different solvent additives.

By considering equation (1) a good agreement between the experimental data and the model, shown by the dashed curves in Figure 1 (a), is found. As evidenced, an active layer modification induced by the solvent mixture has been clearly detected by the noise spectroscopy. The addition of THN solvent to the mixture casues a shifts of f_x to lower frequencies and an increase of K. In Figure 1 (b) the lifetime dependencies on the forward bias voltage, extracted from the noise spectra modeling with $f_x = (2\pi\tau)^{-1}$, for different solvent additives are shown. Devices fabricated by using oDCB show lower values of τ compared to the devices with the blend prepared with oDCB+THN. The addition of THN reduces the recombination rate at the donor-acceptor interface. For a more detailed analysis see.[11] As reported in literature, the charge carrier mobility μ can be extracted from the voltage-noise measurements. [12] The resulting values of μ show an exponential dependence on the square root of the electric field, following the Poole-Frenkel model. [13]

$$\mu = \mu_0 e^{\alpha\sqrt{E}}, \quad (2)$$

where μ_0 is the zero-field mobility, and α is the Poole–Frenkel coefficient. In Figure 1 (c) the mobility dependence on $E^{1/2}$ for the investigated devices is shown. A clear reduction of μ_0 is evident for the devices fabricated with the addition of THN solvent (open symbols) compared to the ones prepared with reference solvent oDCB (full symbols). This is consistent with results reported in literature where the blend casted from a oDCB+THN solvent has a higher polymer crystallinity in the active layer as compared to the blend prepared with oDCB. [14] The main carrier transport mechanism, as already reported in literature for diodes and field effect transistors, is conduction by hopping. [15-17]

Noise characterization of pristine and artificially degraded silicon-based devices

For pristine and artificially degraded silicon solar cells a noise model based on trapping and recombination has been proposed. [6] The variance of the voltage *Var[V]* can be calculated from the experimental data as numerical integration of the noise spectra in the whole investigated frequency range. [6] By varying the light intensity the

experimental data reveals a quadratic dependence of *Var[V]* on R_{rec} indicating that the random current fluctuations $Var[I] = Var[V]/R_{rec}^2$ are constant and do not dependent on the differential resistance value. The amplitude *Var[I]* can be expressed as the sum of dark and photo-induced contribution $Var[I_{dark}]$ and $Var[I_{ph}]$. The observed difference under dark and under illumination has been used to describe the trapping/detrapping and recombination processes within the photovoltaic devices. Therefore, the variance of the current *Var[I]* can be expressed as [6]

$$Var[I] = A_1 \frac{I}{\left(1+\frac{I}{I_0^{light}}\right)^2} + A_2 \frac{I}{\left(1+\frac{I}{I_A}\right)^2} + Var[I_{dark}], \qquad (3)$$

where A_1 and A_2 represent the amplitudes of the current fluctuations due to the recombination and trapping/detrapping mechanisms while $I_0^{light} = \frac{q}{\tau} \cdot A \cdot d \cdot \frac{e_n}{c_n}$ and $I_A = \frac{q}{\tau} \cdot A \cdot d \cdot \frac{N_A}{k}$. Here, A is the device area, d the thickness, N_A the boron doping concentration of the silicon base-material, e_n and c_n the emission and the capture probabilities for the electron traps and k the symmetric ratio of the trap energy level.

Figure 2 (a) shows *Var[I]* as a function of the light intensity for pristine and for irradiated devices. A good agreement between the experimental data and the model described in equation (3) and indicated by the solid curves is found. Under illumination, the $Var[I_{ph}]$ contribution is dominant and is larger than the dark background noise $Var[I_{dark}]$. A further increase of the light intensity causes an increase of the photo-induced noise whose value reaches a saturation level defined as $Var[I]_{sat}$. For the pristine devices the energetic position and the k ratio of the dominant defect centers, extracted by using the noise model in equation (3), can be related to the boron-oxygen complex defect.[6] On the other hand for silicon solar cell, artificially degraded with high energy proton irradiation, the total trap density increases strongly with increasing proton fluence and is also related to a decrease of the power conversion efficiency, as shown in Figure 2 (b) and (c) respectively. It is worth noting that an increase of the trap density corresponds to a proportional increase of the measured noise amplitude.

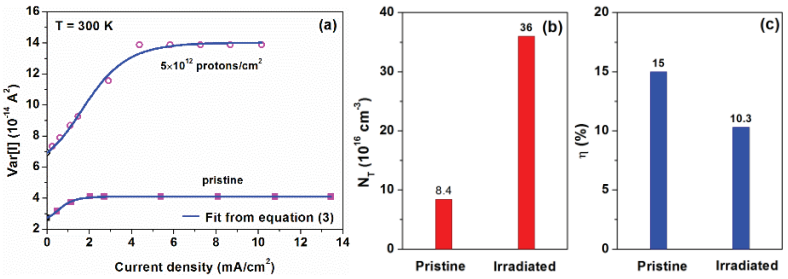

FIGURE 2. (a) Current fluctuation amplitude as a function of the current density at 300 K for a pristine and for proton irradiated silicon solar cell. (b) Defect density and (c) power conversion efficiency values for the pristine and for the irradiated device.

Characterization of perovskite solar cells by low-frequency noise spectroscopy

In Figure 3 (a) the voltage-noise amplitude measured for a perovskite solar cell as a function of the temperature is shown. As evidenced, the noise amplitude gives information about the phase transition between the orthorhombic and the tetragonal crystalline structure of the perovskite at low-temperature showing a peak of the noise amplitude at 160 K.[7] This result is in good agreement with what already reported in literature for the perovskite material.

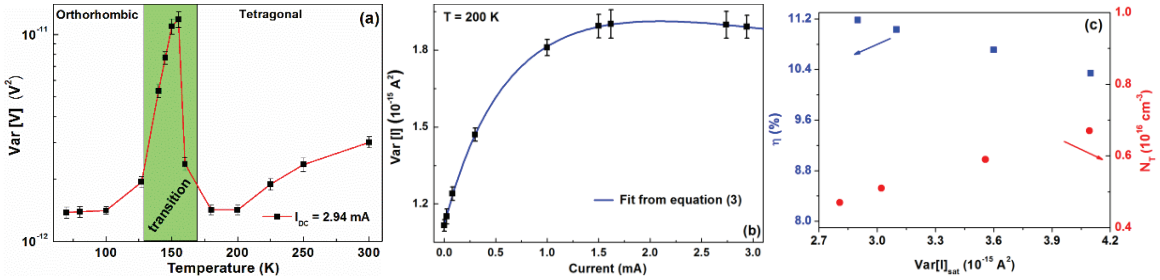

FIGURE 3. (a) Temperature behavior of the voltage-noise amplitude for the perovskite solar cell. (b) Current dependence of the noise amplitude at 200 K. The best fitting curve is shown as blue solid line. (c) Defect density N_T (rigth y-axis) and power conversion efficiency (left y-axis) as a function of the experimental value of $Var[I]_{sat}$.

In the orthorhombic and tetragonal structure the noise amplitude becomes $S_V(f) \approx S_I(f)R_{rec}^2$, whereas, in the phase transition region, the noise is related to the resistance fluctuations. This means that the model of equation (3) can be applied. The current dependence of the noise amplitude for the perovskite solar cell is shown in Figure 3 (b). A good agreement between the best fitting curves (blue solid curve) and the experimental data (full symbols) has been found. The results indicate the presence of band tail states with shallow and deeper traps that influences the solar cell recombination kinetics. In particular, the carrier dynamics is strongly influenced by the electron–phonon interaction. [8] As evidenced in Figure 3 (c), an increase of the trap density N_T in the perovskite causes a decrease of the noise amplitude $Var[I]_{sat}$ with a consequent reduction of the η values.

CONCLUSIONS

The transport and the recombination mechanisms in different photovoltaic devices has been investigated through low-frequency noise spectroscopy. A general trend of the noise amplitude as a function of the charge carrier injection is found. By taking into account trapping/detrapping and recombination phenomena, the electronic transport and defect distribution in the photovoltaic devices can be evaluated. The noise analysis is very sensitive to the morphological and structural modifications occurring in the devices.

ACKNOWLEDGMENTS

The preparation of the organic solar cells by Antonietta De Sio from Oldenburg University and of the perovskite solar cells by Felix Lang from the HZB Berlin is gratefully acknowledged. GL acknowledges financial support from the "VINMAC" project, ID 139455, D. R. Lombardia n. 9559 del 02/08/2017, CUP: E67H16000980009. This work is supported by the CSIR-INDIA and CNR-ITALY Joint Project (2016–2018, 22/CNR/Italy/2016) under Grant CUP: B62F16000090001 and by University of Salerno through grants FARB15PAGAN and FARB17PAGAN.

REFERENCES

1. G. Landi, C. Barone, A. De Sio, S. Pagano, and H.C. Neitzert, Appl. Phys. Lett. **102**, 223902 (2013).
2. C. Barone, G. Landi, C. Mauro, H.C. Neitzert, and S. Pagano, Appl. Phys. Lett. **107**, 143106 (2015).
3. R. Harsh and K.S. Narayan, J. Appl. Phys. **118**, 205502 (2015).
4. S.T. Hsu, Appl. Phys. Lett. **12**, 287 (1968).
5. C. Barone, G. Landi, A. De Sio, H.C. Neitzert, and S. Pagano, Sol. Energy Mater. Sol. Cells **122**, 40 (2014).
6. G. Landi, C. Barone, C. Mauro, H.C. Neitzert, and S. Pagano, Sci. Rep. **6**, 29685 (2016).
7. C. Barone, F. Lang, C. Mauro, G. Landi, J. Rappich, N.H. Nickel, B. Rech, S. Pagano, and H.C. Neitzert, Sci. Rep. **6**, 34675 (2016).
8. G. Landi, H.C. Neitzert, C. Barone, C. Mauro, F. Lang, S. Albrecht, B. Rech, and S. Pagano, Adv. Sci. **4**, 1700183 (2017).
9. A. Guerrero, L.F. Marchesi, P.P. Boix, S. Ruiz-Raga, T. Ripolles-Sanchis, G. Garcia-Belmonte, and J. Bisquert, ACS Nano **6**, 3453 (2012).
10. F.N. Hooge, IEEE Trans. Electron Devices **41**, 1926 (1994).
11. G. Landi, C. Barone, C. Mauro, A. De Sio, G. Carapella, H. Neitzert, and S. Pagano, Energies **10**, 1490 (2017).
12. G. Li, V. Shrotriya, Y. Yao, and Y. Yang, J. Appl. Phys. **98**, 043704 (2005).
13. G. Landi, A.V. Tunc, A. De Sio, J. Parisi, and H.-C. Neitzert, Phys. Status Solidi Appl. Mater. Sci. **213**, (2016).
14. A. De Sio, T. Madena, R. Huber, J. Parisi, S. Neyshtadt, F. Deschler, E. Da Como, S. Esposito, and E. von Hauff, Sol. Energy Mater. Sol. Cells **95**, 3536 (2011).
15. V. V. Brus, F. Lang, J. Bundesmann, S. Seidel, A. Denker, B. Rech, G. Landi, H.C. Neitzert, J. Rappich, and N.H. Nickel, Adv. Electron. Mater. **3**, 1600438 (2017).
16. G. Landi, W.R. Fahrner, S. Concilio, L. Sessa, and H.C. Neitzert, IEEE J. Electron Devices Soc. **2**, 179 (2014).
17. G. Landi, A.V. Tunc, A. De Sio, J. Parisi, and H.-C. Neitzert, Phys. Status Solidi **213**, 1909 (2016).